A unified mapping framework of multifaceted pharmacodynamic responses to hypertension interventions

Qian Wang[1], Jingwen Gan[1], Kun Wei[1], Scott A. Berceli[2,3,4], Claudia Gragnoli[5,6,7] and Rongling Wu[1,6,8]

[1] Center for Computational Biology, College of Biological Sciences and Technology, Beijing Forestry University, Beijing 100083, China
[2] Malcom Randall VA Medical Center, Gainesville, FL 32610, USA
[3] Department of Surgery, University of Florida, Box 100128, Gainesville, FL 32610, USA
[4] Department of Biomedical Engineering, University of Florida, Gainesville, FL 32610, USA
[5] Division of Endocrinology, Diabetes, and Metabolic Disease, Translational Medicine, Department of Medicine, Sidney Kimmel Medical College, Thomas Jefferson University, Philadelphia, PA 19107, USA
[6] Department of Public Health Sciences, Penn State College of Medicine, Hershey, PA 17033, USA
[7] Molecular Biology Laboratory, Bios Biotech Multi Diagnostic Health Center, Rome 00197, Italy
[8] Center for Statistical Genetics, Departments of Public Health Sciences and Statistics, Pennsylvania State University, Hershey, PA 17033, USA

The personalized therapy for hypertension needs comprehensive knowledge about how blood pressures (BPs; systolic and diastolic) and their pulsatile and steady components are controlled by genetic factors. Here, we propose a unified pharmacodynamic (PD) functional mapping framework for identifying specific quantitative trait loci (QTLs) that mediate multivariate response–dose curves of BP. This framework can characterize how QTLs govern pulsatile and steady components through jointly regulating systolic and diastolic pressures. The model can quantify the genetic effects of individual QTLs on maximal drug effect, the maximal rate of drug response, and the dose window of maximal drug response. This unified mapping framework provides a tool for identifying pharmacological genes potentially useful to design the right medication and right dose for patients.

Introduction

Systolic blood pressure (SBP) and diastolic blood pressure (DBP), reflecting roughly the peak and trough of BP, are commonly used as a criterion to diagnose and evaluate hypertension and its severity, and to predict hypertension-related comorbidities [1,2]. A growing body of evidence shows that the association of BP with the risk of cardiovascular disease is determined not only by either SBP or DBP, but also by the pulsatile component (described by pulse pressure, PP) and the steady component (described by mean arterial pressure, MAP) [3–9]. Several studies have characterized hemodynamic determinants of these two components and the physiological mechanisms of how they impact heart function and disease [8–10]. The pulsatile component is determined by ventricular ejection fraction, large-artery stiffness, early pulse-wave reduction, and heart rate [11], whereas the steady component is affected by left ventricular contractility, heart rate, and vascular resistance and elasticity averaged over time [3]. Current diagnostic protocols have used SBP and/or DBP, in conjunction with MAP and PP, to more comprehensively assess hypertension-related health risk [6]. For pharmacy sectors, an essential task is to develop and deliver specific medications for the simultaneous intervention for abnormal SBP and DBP as well as for PP and MAP according to patients' genetic make-ups. Unfortunately, this is difficult because of the inconsistent responses of different BP measures to drugs and to different patterns of how genes control these BP-related drug responses.

Previous studies through genetic mapping and genome-wide association mapping have identified important QTLs that affect MAP and PP in animal and human populations [12–15]. In a meta-analysis of 150 134 individuals from 54 genome-wide association

Corresponding author: Wu, R. (rwu@bjfu.edu.cn), (rwu@phs.psu.edu)

1359-6446/
https://doi.org/10.1016/j.drudis.2019.01.009

studies (GWAS) of European ancestry with 1000 Genomes Project-based imputation, Wain *et al.* [16] identified a total of 48 genes that are involved in differences of SBP, DBP, and PP among humans. Chauvet *et al.* [17] found that QTLs affect the MAP of the inbred rat through modularity and epistasis. However, current studies of BP genetics are limited from a pharmacological perspective. First, these studies have not integrated the MAP- and/or PP-related drug response, limiting the discovery of genetic loci influencing BP improvement through drugs. Second, the MAP and PP responses to drugs are a dynamic process that follows PD and pharmacokinetic (PK) principles of drug effects and absorption in the body [18,19]. The incorporation of PD and PK processes can enhance our understanding of the mechanistic basis of drug response.

Here, we propose and assess a genetic mapping framework of BP that incorporates PD principles into a pharmacogenetic trial. The advantages of PD modeling to study pharmacogenetics have been well recognized in previous studies. Wu and his group implemented dynamic mapping, called functional mapping, to map pharmacogenetic loci for drug response [20–23]. This model was then conceptualized as a theory for computational pharmacogenetics and pharmacogenomics [24–26], which has been effectively used in practice. For example, Mustavich *et al.* [27] used it to detect loci that control susceptibility to alcohol dependence, and Wang *et al.* [28] applied it to identify important pharmacological genes for glucocorticoid intervention in asthma. This theory can be extended to model how SBP and DBP respond differently to drugs and how their derived variables, MAP and PP, are dynamically related in terms of drug treatments. We also review a statistical procedure for mapping and identifying specific QTLs that govern MAP and PP curves, and outline several clinically meaningful hypothesis tests used to address how a QTL determines the key events of PD and PK processes. We validate the model by analyzing a set of real data from dobutamine pharmacological studies.

A unified framework of functional mapping

Clinical pharmacogenetic trials

GWAS have been increasingly used to investigate the pharmacogenetic mediation of drug response. A particular GWAS includes n patients who differ in age, race, sex, body mass index (BMI), and other demographic factors, recruited from a general population. These demographic factors are treated as covariates of drug response. Consider a drug that can control BP and PP. The drug is administered to each patient by a series of physiologically tolerable doses (C_1, . . . , C_T), at each of which both SBP and DBP are monitored. Let $\mathbf{x}_{1i} = [x_{1i}(C_1), \ldots, x_{1i}(C_T)]$ and $\mathbf{x}_{2i} = [x_{2i}(C_1), \ldots, x_{2i}(C_T)]$ denote the vectors of SBP and DBP values for subject i, respectively. MAP ($\mathbf{y}_i$) is approximated by one-third of SBP plus two-thirds of DBP at normal resting heart rates, whereas PP ($\mathbf{z}_i$) of this subject is defined as the difference between DBP and SBP[5]. Then, we have Eqs (1a) and (1b):

$$\mathbf{y}_i = [x_{1i}(C_1) + 2x_{2i}(C_1), \ldots, x_{1i}(C_T) + 2x_{2i}(C_T)]/3 \quad (1a)$$

$$\mathbf{z}_i = [x_{1i}(C_1) - x_{2i}(C_1), \ldots, x_{1i}(C_T) - x_{2i}(C_T)] \quad (1b)$$

These two derived variables are used to map BP QTLs. All the patients who participated in this study are genome-wide genotyped for thousands of thousands of single nucleotide polymorphisms (SNPs), at each of which there are three different genotypes *AA*, *Aa*, and *aa*. Let n_1, n_2, and n_3 denote the observations of the three genotypes, respectively.

The drug-induced biochemical and distribution effects in the human body obey some basic kinetic rules that can be described by PD and PK equations. The Emax model is one of the most commonly used PD models to illustrate and quantify drug dose-effect relationship (Eq. (2)):

$$E = E_0 + \frac{E_{\max} C^H}{EC_{50}^H + C^H} \quad (2)$$

where E is the drug effect at dose C, E_0 is the baseline, $E_{\max}$ is the asymptotic (limiting) effect, EC_{50} is the drug concentration that results in 50% of the maximal effect, and H is the slope parameter that determines the slope of the dose–response curve. The larger H, the steeper the linear phase of the log-dose-effect curve. In practice, to reduce the number of curve parameters being estimated, we can remove the baseline effect E_0 by normalizing the longitudinal data.

Likelihood and estimation

To map BP QTLs, we formulate the likelihood of derived variables (1a) and (1b) at a given QTL using Eq. (3):

$$L(\mathbf{y}, \mathbf{z}) = \prod_{i=1}^{n_1} f_1(y_i, z_i) \prod_{i=1}^{n_2} f_2(y_i, z_i) \prod_{i=1}^{n_3} f_3(y_i, z_i)$$

where $f_j(\mathbf{y}_i, \mathbf{z}_i)$ is a bivariate longitudinal normal distribution for genotype j (j = 1 for *AA*, 2 for *Aa* and 3 for *aa*). This distribution has a form calculated using Eq. (4):

$$f_j(y_i, z_i) = \frac{1}{(2\pi)^T |\boldsymbol{\Sigma}|^{\frac{1}{2}}} \exp\left[-\frac{1}{2}\left(y_i - \boldsymbol{\mu}_{j|i}^{y}\right) \boldsymbol{\Sigma}^{-1} \left(z_i - \boldsymbol{\mu}_{j|i}^{z}\right)\right] \quad (4)$$

which is specified by the vectors of overall genotypic means for subject i who carries genotype j for two BP parameters, SBP and DBP, and the SBP and DBP covariance matrix. The overall genotypic mean vectors are defined using Eqs (5a) and (5b):

$$\mu_{j|i}^{y} = \left\{ \begin{array}{l} \frac{E_{\max j}^{S} C_\tau^{H_{Sj}}}{3(EC_{50j}^{H_{Sj}} + C_\tau^{H_{Sj}})} + \sum_{r=1}^{R} \alpha_r^S u_{ir}^S + \sum_{h=1}^{H} \sum_{l=1}^{L_h} \xi_{ihl} v_{hl}^S + \\ \frac{2E_{\max j}^{D} C_\tau^{H_{Dj}}}{3(EC_{50Dj}^{H_{Dj}} + C_\tau^{H_{Dj}})} + \sum_{r=1}^{R} \alpha_r^D u_{ir}^D + \sum_{h=1}^{H} \sum_{l=1}^{L_h} \xi_{ihl} v_{hl}^D \end{array} \right\}_{\tau=1}^{T} \quad (5a)$$

$$\mu_{j|i}^{z} = \left\{ \begin{array}{l} \frac{E_{\max j}^{S} C_\tau^{H_{Sj}}}{EC_{50j}^{H_{Sj}} + C_\tau^{H_{Sj}}} + \sum_{r=1}^{R} \alpha_r^S u_{ir}^S + \sum_{h=1}^{H} \sum_{l=1}^{L_h} \xi_{ihl} v_{hl}^S \\ -\frac{E_{\max j}^{D} C_\tau^{H_{Dj}}}{EC_{50Dj}^{H_{Dj}} + C_\tau^{H_{Dj}}} - \sum_{r=1}^{R} \alpha_r^D u_{ir}^D - \sum_{h=1}^{H} \sum_{l=1}^{L_h} \xi_{ihl} v_{hl}^D \end{array} \right\}_{\tau=1}^{T} \quad (5b)$$

Eqs (5a) and (5b) include two parts: the first is the genotypic value specified by the E_0-removed Emax model and the second is the effect resulting from variate covariates. The E_0-removed Emax model is defined by the parameters ($E_{\max j}^S$, E_{50Sj}, H_{Sj}) for the SBP curve and ($E_{\max j}^D$, E_{50Dj}, H_{Dj}) for the DBP curve at genotype j. The covariate model specifies the effect of continuous and discrete covariates on SBP and DBP, respectively, including u_{ir} (r = 1, . . . , R), the value of the rth continuous covariate, such as age and BMI, for subject i; α_r, the effect of the rth continuous covariate; v_{sl} (l = 1, . . . , L_s, s = 1, . . . , S), the effect of the lth level for the sth discrete covariate, such as race, gender, and treatment, with $\sum_{l=1}^{L_s} v_{sl} = 0$,

where L_s is the number of levels for the sth discrete covariate; and ξ_{isl} is an indicator variable of subject i who receives the lth level of the sth discrete covariate.

The longitudinal covariance matrix Σ_i of Eq. (4) contains covariance matrices within and between two BP parameters. A variety of statistical approaches have been proposed to model the covariance structure. These approaches can be parametric, such as autoregressive, antedependent, autoregressive moving average, Brownian motion, and Ornstein–Uhlenbeck processes, and also nonparametric, such as B-spline and Legendre orthogonal polynominals. A model selection procedure is implemented to determine an optimal order of each approach and then the most parsimonious approach for covariance modeling [29–31].

To obtain the maximum-likelihood estimates (MLEs) of the unknown parameters in Eq. (4), a hybrid of the Nelder–Mead Simplex and least squares methods can be implemented. The MLEs of the covariate effects are obtained by a least-square method, whereas the Emax parameters of three genotypes ($E^S_{\text{max}j}$, E_{50Sj}, H_{Sj} and $E^D_{\text{max}j}$, E_{50Dj}, H_{Dj}) and covariance-structuring parameters are estimated by the Simplex method.

Hypothesis tests

We provide a platform to test several hypotheses regarding the genetic control of how BP parameters respond to drug intervention. To test whether a significant QTL for BP exists, the following hypotheses are formulated (Eq. (6)):

$$\begin{aligned} H_0 &: \left(E^S_{\text{max}j}, E_{50Sj}, H_{Sj}\right) \\ &\equiv (E^S_{\text{max}}, E_{50S}, H_S) \text{ and } (E^D_{\text{max}j}, E_{50Dj}, H_{Dj}) \\ &\equiv (E^D_{\text{max}}, E_{50D}, H_D) \end{aligned} \tag{6}$$

H_1: at least one of the equalities above does not hold for any $j = 1, 2, 3$.

By calculating the log-likelihood ratio of H_0 and H_1, we can claim whether a significant QTL has been detected. This can be done by comparing this ratio against the critical threshold determined by permutation tests.

Next, it is important to test how the QTL affects MAP and PP. This can be done by formulating the following null hypotheses (Eqs (7) and (8)):

$$\begin{aligned} H_0 &: \frac{E^S_{\text{max}j} C_\tau^{H_{Sj}}}{3(EC^{H_{Sj}}_{50Sj} 1 C_\tau^{H_{Sj}})} 1 \frac{2E^D_{\text{max}j} C_\tau^{H_{Dj}}}{3(EC^{H_{Dj}}_{50Dj} 1 C_\tau^{H_{Dj}})} \\ &\equiv \frac{E^S_{\text{max}} C_\tau^{H_S}}{3(EC^{H_S}_{50S} 1 C_\tau^{H_S})} 1 \frac{2E^D_{\text{max}} C_\tau^{H_D}}{3(EC^{H_D}_{50D} 1 C_\tau^{H_D})} \end{aligned} \tag{7}$$

$$H_0 : \frac{E^S_{\text{max}j} C_\tau^{H_{Sj}}}{EC^{H_{Sj}}_{50Sj} 1 C_\tau^{H_{Sj}}} - \frac{E^D_{\text{max}j} C_\tau^{H_{Dj}}}{EC^{H_{Dj}}_{50Dj} 1 C_\tau^{H_{Dj}}} \equiv \frac{E^S_{\text{max}} C_\tau^{H_S}}{EC^{H_S}_{50S} 1 C_\tau^{H_S}} - \frac{E^D_{\text{max}} C_\tau^{H_D}}{EC^{H_D}_{50D} 1 C_\tau^{H_D}} \tag{8}$$

If both these null hypotheses are rejected, this means that this QTL pleiotropically determines MAP and PP. Otherwise, this QTL might be specific for one of the two traits.

We can also test how the QTL governs DBP and SBP. These tests can be based on the comparison of Hill coefficients among genotypes. Specifically, we have (Eq. (9)):

$$H_0 : (E^S_{maxj}, E_{50Sj}, H_{Sj}) \equiv (E^S_{max}, E_{50S}, H_S) \tag{9}$$

$$H_0 : (E^D_{maxj}, E_{50Dj}, H_{Dj}) \equiv (E^D_{max}, E_{50D}, H_D) \tag{10}$$

If both these null hypotheses are rejected, this implies that the QTL is pleiotropic, triggering an effect on both DBP and SBP. Otherwise, it only affects one of the two BP parameters.

We can systematically characterize the genetic control of drug response as a dynamic process through BP parameters and their derived variables, which are physiologically meaningful. The additional advantages of this model lie in its capacity to detect the genetic basis of key events that have a central role in the outcome of drug efficacy. Based on the Emax model (Eq. (1)), this model can test how the QTL determines maximum drug effect (E_{max}), the dose at which the drug effect achieves half of its maximal value (EC_{50}), the slope of drug response curve (H), and the dose at which the drug–response change rate is maximal (C_I), expressed as Eq. (11):

$$C_I 5 \left[\frac{(H-1)EC_{50}^H}{H11}\right]^{\frac{1}{H}} \tag{11}$$

We might be interested in testing genetic differences at any dose estimate, EC_p, which is the dose generating p-percentile of E_{max}, as an estimate of the maximal effective dose. For example, EC_{90} is of interest in dose–response analysis. EC_p is calculated using Eq. (12):

$$EC_p 5 EC_{50} \left(\frac{p}{1-p}\right)^{\frac{1}{H}} \tag{12}$$

All these tests can be established on both DBP and SBP parameters.

Haplotype mapping

Previous mapping studies with these data suggest that haplotype variants are a better determinant of pharmacological response to drugs than are individual SNPs. As such, we also incorporated the haplotype model into Eq. (3). Consider a pair of SNPs with alleles A versus a, and B versus b, respectively, which form four possible haplotypes AB, Ab, aB, and ab with frequencies estimated from the EM algorithm [20]. The haplotype model states that differences among these haplotypes are one of the causes of the phenotypic variation of a complex trait [32]. We used a risk haplotype to define a haplotype that is different from the remaining haplotypes. If AB is a risk haplotype and $\overline{AB}$ is the collective set of all remaining haplotypes, we can expect that diplotypes $AB|AB$, $AB|\overline{AB}$, and $\overline{AB}|\overline{AB}$ perform differently. It is possible to distinguish $AB|AB$, $\overline{AB}|\overline{AB}$, and most types of $AB|\overline{AB}$ directly from the genotype data. However, an individual carrying the double heterozygote genotype $AaBb$ can be either diplotype $AB|ab$ or diplotype $Ab|aB$, which cannot be directly distinguished from each other. Lin *et al.* [20] implemented the EM algorithm to distinguish these two diplotypes so that their effect on drug response can be estimated. By assuming each haplotype as a risk haplotype, we estimated the likelihood value from Eq. (3). The optimal risk haplotype can be inferred from information criteria AIC. The processes of covariance-structuring parameter estimation and hypothesis tests for haplotype mapping follow those for locus mapping.

Model application

To validate the utility of our model, we analyzed a pharmacogenetic data of cardiovascular disease [20]. The study included a group of 163 patients from age 32 to 86 years, treated with

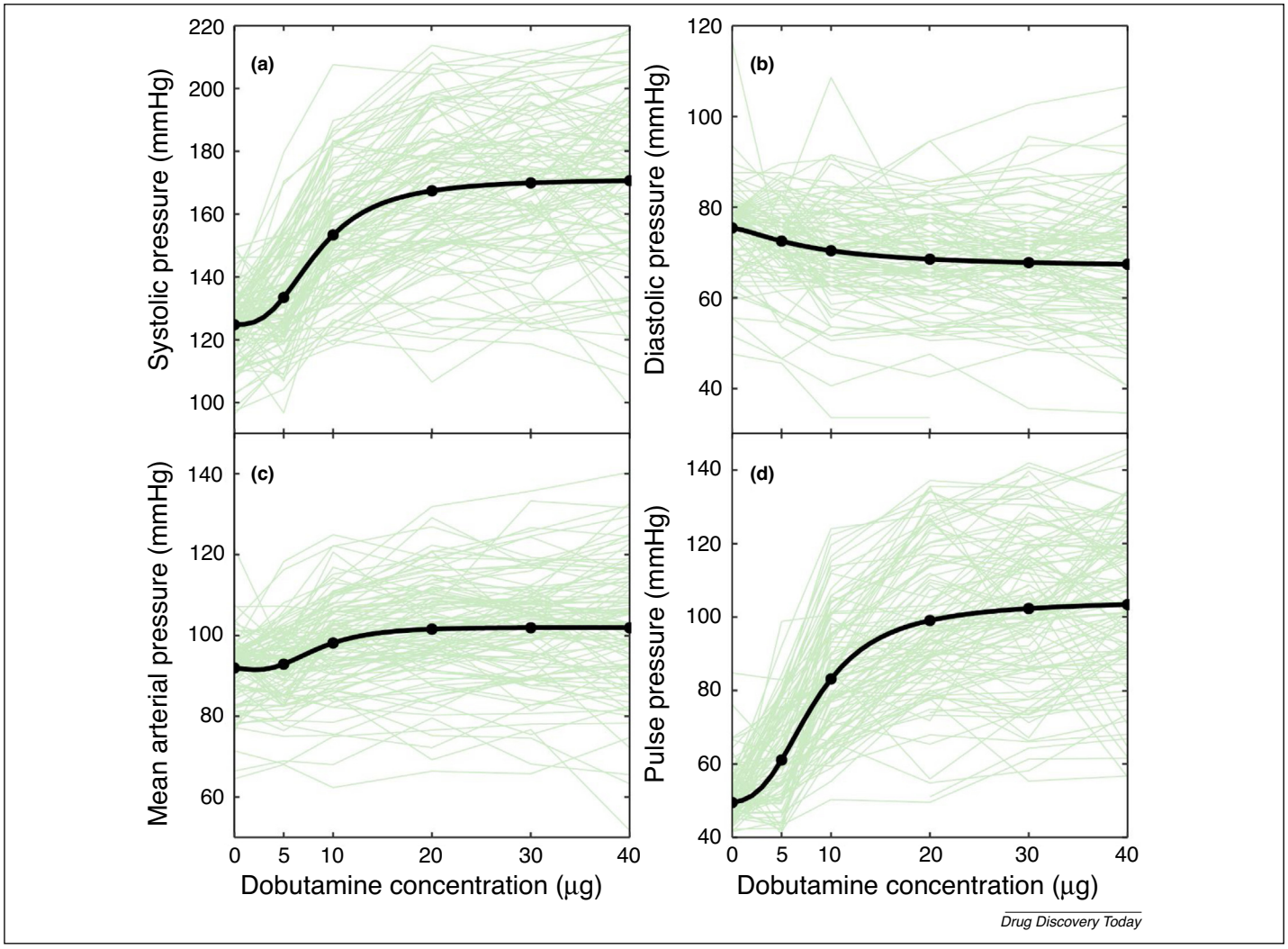

FIGURE 1

Response curves for systolic blood pressure (SBP) (**a**) and diastolic blood pressure (DBP) (**b**) to dobutamine in a pharmacogenomic study comprising 107 patients. From SBP and DBP, we obtained the curves of mean arterial pressure (MAP) (**c**) and pulse pressure (PP) (**d**). Thin green lines are response curves of individual subjects, and thick black lines are the mean curves fitted by the Hill equation. Dots are the doses of dobutamine at which SBP and SBP were measured.

dobutamine, a medication able to control by intravenous administration acute congestive heart failure by increasing heart rate and cardiac contractility. The patients had a range of baseline (untreated) heart rates. The patients received increasing doses of dobutamine, from 0 (baseline) to 5, 10, 20, 30, and 40 μg, at each of which their heart rates were recorded. The maximum doses varied among subjects because of different physiological limits (e.g., age, BMI, or baseline heart rate). Dobutamine is a synthetic catecholamine with an important role in enhancing cardiac inotropic function by primarily stimulating sympatichomimetic β_1-adrenergic receptors (β_1AR) and, thus, increasing contractility and cardiac output. Dobutamine has also weak sympatichomimetic β_2 activity, promoting target organ artery vasodilation, and sympatichomimetic α_1 selective activity increasing BP. This study genotyped five SNPs, two located at codons 49 (Ser49Gly) and 389 (Arg389Gly) within the *b1AR* gene, two situated at codons 16 (Arg16Gly) and 27 (Gln27Glu) within the β_2-adrenergic receptor (*b2AR*) gene, and one found at codon 492 (Arg492Cys) within the α_1-adrenergic receptor (*a1AR*) gene. Here, we test whether these SNPs are associated with BP parameters.

We first corrected dobutamine dose-dependent heart-rate data by removing the effects resulting from age, sex, race, and BMI. By plotting all subjects' SBP and DBP values against different doses of dobutamine, we found different patterns of change between these two BP measures. In general, SBP increased with dose (Fig. 1a), whereas DBP decreased with dose (Fig. 1b). The average curves of both SBP and DBP can be fitted by the Hill equation (Adjusted $R^2 > 0.098$). By incorporating the Hill equation into Eqs. (1a) and (1b), we estimated the average curves of MAP (Fig. 1C) and PP (Fig. 1D). Both MAP and PP increased with dose, although the PP dose-related increase was expected given the dose-dependent SBP augmentation and DBP reduction. PP also had a greater rate of change than MAP. Comparisons among SBP, DBP, MAP, and PP suggested divergent patterns by which these four types of BP measure respond to dobutamine. By associating individual SNPs with BP measures through the unified mapping model, we tested

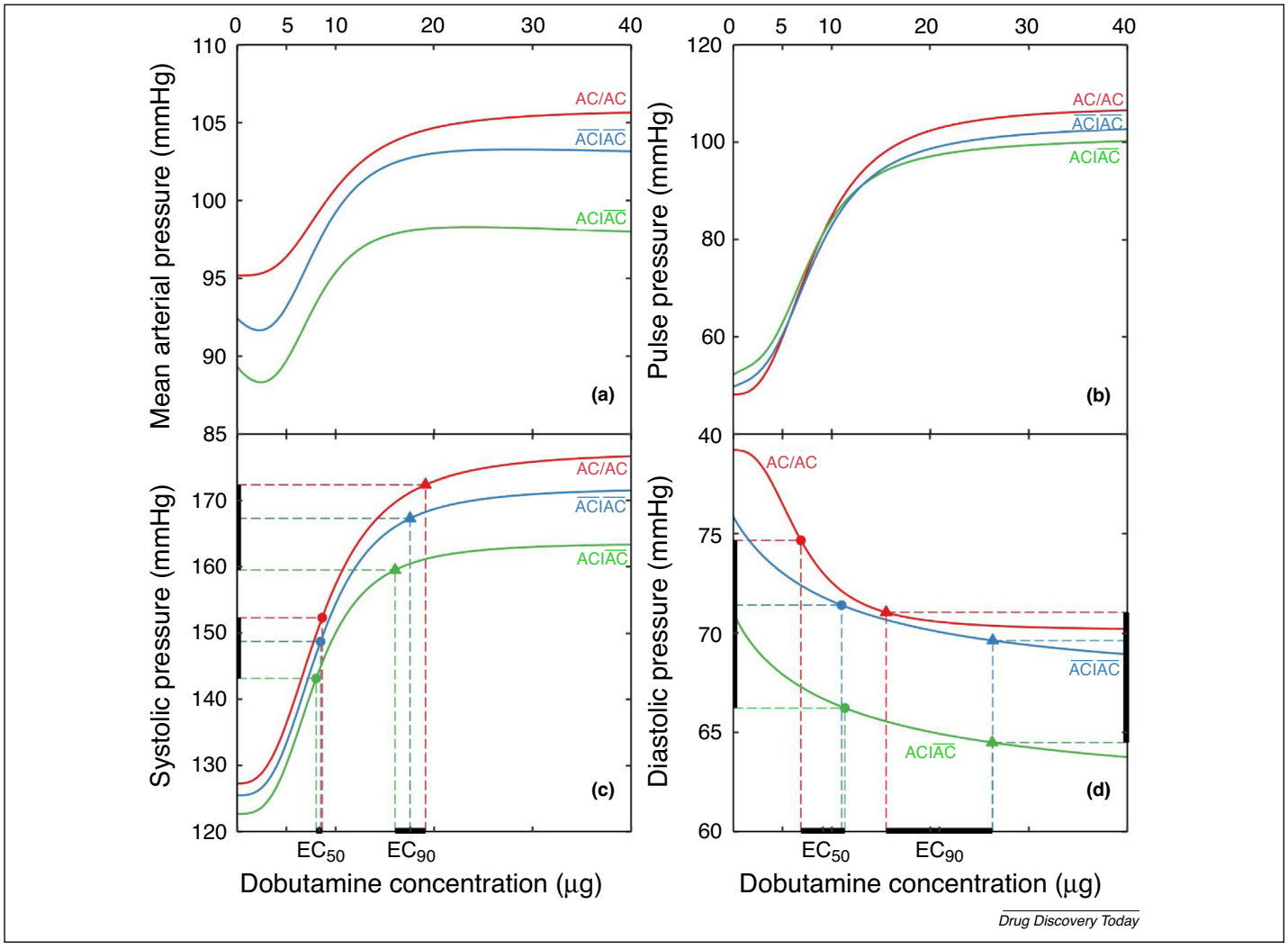

FIGURE 2

Genetic curves of mean arterial pressure (MAP) (**a**) and blood pressure (**b**) in terms of three diplotypes ($AC|AC$, $AC|\overline{AC}$, and $\overline{AC}|\overline{AC}$) between two single nucleotide polymorphisms (SNPs) within the *b1AR* gene, estimated from the likelihood (see Eq. (2) in the main text). The estimated Hill coefficients were used to draw systolic blood pressure (SBP) (**a**) and diastolic blood pressure (DBP) curves (**b**) for each diplotype. The doses at which the drug response reaches half of the maximum effect (EC_{50}, solid circles) and 90% of maximum effect (EC_{90}, solid triangles) are indicated.

the significance of each association. We did not find significant SNPs that jointly affect different BP measures.

By testing each pair of SNPs from the same gene, the haplotype model identified a significant risk haplotype AC within the *b1AR* gene for BP parameters in response to dobutamine (Fig. 2). This haplotype affects MAP and PP in two ways. First, diplotypes ($AC|AC$, $AC|\overline{AC}$), which contain at least one copy of the risk haplotype, are dramatically different from the haplotypes ($\overline{AC}|\overline{AC}$), which do not contain the risk haplotype ($P < 0.01$; Fig. 2a,b). Second, and more interestingly, diplotype ($AC|AC$) with two copies of the risk haplotype differs at an even higher significance level ($P < 0.001$) from diplotype ($AC|\overline{AC}$) with one copy of the risk haplotype. These results indicate that risk haplotype AC mediates MAP and PP not only through its existence, but also through its frequency and interaction with nonrisk haplotypes. Over the whole dobutamine-dose levels considered, diplotype $AC|AC$ correlated consistently with a larger MAP value than did the other two diplotypes, whereas the diplotype $\overline{AC}|\overline{AC}$ correlated consistently with a larger MAP than did $AC|\overline{AC}$. This suggests that the risk haplotype AC, by its interaction effect with the other haplotypes, reduces MAP more effectively than the dobutamine dose can increase it (Fig. 2a).

Compared with MAP, PP was found to be more sensitive to dobutamine (Fig. 2b). Starting at a lower BP increment level (~50 mmHg), among three diplotypes, $AC|AC$ reached the largest PP (>100 mmHg) increment at a medium–high dose of dobutamine because of its highest slope of PP response to dobutamine. Among three diplotypes, diplotype $AC|\overline{AC}$ had the lowest slope, suggesting that the interaction between risk haplotype AC and any of the other haplotypes inhibits the response of PP to dobutamine. Using the diplotype-dependent estimates of Hill coefficients from the likelihood estimate (Eq. (2)), We drew the curves of SBP and DBP (Fig. 2c,d) from which we found that, among the three diplotypes, diplotype $AC|AC$ exhibited the highest SBP and DBP over the entire range of dobutamine doses. Diplotype $AC|\overline{AC}$ had the lowest SBP and DBP, suggesting again the interaction between the risk haplotype AC and the other haplotypes as a crucial determinant of BP parameters.

We further dissected the pattern of how the risk haplotype governs BP. Three diplotypes started from slightly different baselines of SBP and displayed small differences in the dose reaching a half of maximum drug effect (EC_{50}), but diverged dramatically in the persistence to response to dobutamine (Fig. 2C). Despite a smaller slope ($H = 2.77$), $AC|AC$ reached 90% of maximum drug effect at a larger dose (EC_{90}), compared with diplotypes $\overline{AC}|\overline{AC}$ ($H = 3.02$) and $AC|\overline{AC}$ ($H = 3.17$). Unlike SBP, DBP exhibited remarkable differences among three diplotypes over an entire range of dobutamine doses (Fig. 2d). Starting from a larger DBP baseline, diplotype $AC|AC$ was more responsive to dobutamine, at a greater steepness ($H = 2.69$) than diplotypes $\overline{AC}|\overline{AC}$ ($H = 0.98$) and $AC|\overline{AC}$ ($H = 0.89$). The three diplotypes differed strikingly in the dose reaching a half of the maximum drug effect, whereas the difference in the dose at 90% of maximum drug effect was even more pronounced.

Concluding remarks

Increasing evidence from large-scale epidemiological cohort studies has shown that the difference of SBP from DBP, defined as PP, reflecting arterial stiffness, and two-thirds of DBP plus one-third of SBP, defined as MAP, reflecting left ventricular contractility and heart rate, are highly associated with heart function, disease, and aging [7–10,15]. Genetic studies have demonstrated the genetic variation of PP and MAP [12–14], suggesting that the influences of these two BP traits on heart dysfunction vary interindividually. As such, it is essential to investigate the genetic basis of these BP parameter responses to drug interventions, which should be based on personalized medicine, to best prevent and treat cardiovascular disease, thereby improving quality of life and prolonging life expectancy.

We argue that a unified functional mapping framework is powerful for identifying, visualizing, and quantifying the genetic architecture of PP- and MAP-related drug responses. This framework integrates the PD principle of drug response into a mapping or association setting through mathematical equations. It is characterized by three features. First, by taking advantages of PD, hemodynamics, genetics, and statistics, the framework can map individual QTLs for the pharmacological response of PP and MAP. Second, the framework can demonstrate and test whether and how PP and MAP are governed jointly by the same set of QTLs. Results from this testing are important for stratifying patients and tailoring therapy based on how the patients respond to PP and MAP treatments. Third, the framework enables the testing of several clinically meaningful hypotheses regarding pharmacological reactions and metabolism. It can identify and quantify how some key events of drug response affect drug-effect outcome.

The mapping framework focuses on the genetic effect of DNA sequence variants on drug response, but many other sources, such as genetic imprinting and epigenetic modifications, might have an important role in moderating drug efficacy. Genetic imprinting can be incorporated into the model by recruiting the DNA information of patients' parents. Li and Wu [33] developed a model that can jointly analyze genetic data from parents and their offspring. This model was able to estimate in a case-control [34] and population-based cohort study [35] the genetic influences and the genetic imprinting effects at the same QTLs. These extensions can be readily implemented into our model, allowing joint testing of genetic influences as well as genetic imprinting effects. Second, as a demonstration, we assumed a single marker analysis, which cannot estimate epistatic effects per se. Multi-locus models can be developed, allowing the genetic architecture of drug responses to be dissected in terms of genetic interactions [17]. Third, marginal single marker genetic analysis might be limited in charting an overall picture of genetic control mechanisms among all loci. Variable selection has been implemented to analyze all possible markers simultaneously and to further select and estimate a sparse set of loci for complex traits in genetic mapping or association studies of dynamic traits [36–38]. This statistical procedure can be readily merged with our model, which will help to systematically illustrate and characterize the pharmacogenetic control over PP and MAP. We have packed all statistical estimation and tests into BPmap freely available upon request from the corresponding author.

Acknowledgments

This study was supported by Fundamental Research Funds for the Central Universities (NO. 2015ZCQ-SW-06) and grants U01 HL119178 (S.B. and R.W.) and NICHD 5R01HD086911-02 (C.G. and R.W.) from the National Institute of Health.

References

1 Joint National Committee on the Detection, Evaluation, Treatment of High Blood Pressure (1997) The sixth report of the Joint National Committee on prevention, detection, evaluation, and treatment of high blood pressure. *Arch. Intern. Med.* 157, 2413–2446

2 Sesso, H.D. *et al.* (2000) Systolic and diastolic blood pressure, pulse pressure, and mean arterial pressure as predictors of cardiovascular disease risk in men. *Hypertension* 36, 801–817

3 Safar, M.E. (1989) Pulse pressure in essential hypertension: clinical and therapeutical implications. *J. Hypertens.* 7, 769–776

4 Darne, B. *et al.* (1989) Pulsatile versus steady component of blood pressure: a cross-sectional analysis and a prospective analysis on cardiovascular mortality. *Hypertension* 13, 392–400

5 Domanski, M.J. *et al.* (1999) Isolated systolic hypertension: prognostic information provided by pulse pressure. *Hypertension* 34, 375–380

6 Palaniappan, L. *et al.* (2002) Comparison of usefulness of systolic, diastolic, and mean blood pressure and pulse pressure as predictors of cardiovascular death in patients ≥60 years of age (The Dubbo Study). *Am. J. Cardiol.* 90, 1398–1401

7 Larstorp, A.C. *et al.* (2012) Association of pulse pressure with new-onset atrial fibrillation in patients with hypertension and left ventricular hypertrophy: the Losartan Intervention For Endpoint (LIFE) reduction in hypertension study. *Hypertension* 60, 347–353

8 Dart, A.M. (2017) Should pulse pressure influence prescribing? *Aust. Prescr.* 40, 26–29

9 Melo, X. *et al.* (2018) Pulse pressure tracking from adolescence to young adulthood: contributions to vascular health. *Blood Press.* 27, 19–24

10 Vennin, S. *et al.* (2016) Identifying hemodynamic determinants of pulse pressure a combined numerical and physiological approach. *Hypertension* 70, 1176–1182

11 Franklin, S.S. *et al.* (1997) Hemodynamic patterns of age-related changes in blood pressure: the Framingham Heart Study. *Circulation* 96, 308–315

12 Wain, L.V. *et al.* (2011) Genome-wide association study identifies six new loci influencing pulse pressure and mean arterial pressure. *Nat. Genet.* 43, 1005–1011

13 Hong, K.W. *et al.* (2012) Recapitulation of genome-wide association studies on pulse pressure and mean arterial pressure in the Korean population. *J. Hum. Genet.* 57, 391–393

14 Koh-Tan, H.H. *et al.* (2017) Dissecting the genetic components of a quantitative trait locus for blood pressure and renal pathology on rat chromosome 3. *J. Hypertens.* 35, 319–329

15 Padmanabhan, S. and Joe, B. (2017) Towards precision medicine for hypertension: a review of genomic, epigenomic, and microbiomic effects on blood pressure in experimental rat models and humans. *Physiol. Rev.* 97, 1469–1528

16 Wain, L.V. *et al.* (2017) Novel blood pressure locus and gene discovery using genome-wide association study and expression data sets from blood and the kidney. *Hypertension* 70, e4–e19

17 Chauvet, C. *et al.* (2013) Modularization and epistatic hierarchy determine homeostatic actions of multiple blood pressure quantitative trait loci. *Hum. Mol. Genet.* 22, 4451–4459

18 Giraldo, J. (2003) Empirical models and Hill coefficients. *Trends Pharm. Sci.* 24, 63–65

19 Wang, Y.Q. *et al.* (2013) Delivering systems pharmacogenomics towards precision medicine through mathematics. *Adv. Drug Deliv. Rev.* 65, 905–911

20 Lin, M. *et al.* (2005) Sequencing drug response with HapMap. *Pharmacogenomics J.* 5, 149–156

21 Lin, M. *et al.* (2006) A bivariate functional mapping model for gene identification of drug response for systolic and diastolic blood pressures. *Pac. Symp. Biocomput.* 11, 572–583

22 Lin, M. *et al.* (2007) Modeling sequence-sequence interactions for drug response. *Bioinformatics* 23, 1251–1257

23 Lin, M. *et al.* (2010) Modeling the genetic etiology of pharmacokinetic-pharmacodynamic links with the ARMA process. *J. Biopharm. Stat.* 20, 351–372

24 Wu, R.L. and Lin, M. (2008) *Statistical and Computational Pharmacogenomics*. Chapman & Hall/CRC

25 Ahn, K. *et al.* (2010) Functional mapping of drug response with pharmacodynamic-pharmcokinetic principles. *Trends Pharmacol. Sci.* 31, 306–311

26 Wu, R.L. *et al.* (2011) A conceptual framework for integrating pharmacodynamic principles into genome-wide association studies for pharmacogenomics. *Drug Discov. Today* 16, 884–890

27 Mustavich, L.F. *et al.* (2010) Using a pharmacokinetic model to relate an individual's susceptibility to alcohol dependence to genotypes. *Hum. Hered.* 70, 177–193

28 Wang, Y.Q. *et al.* (2015) Pharmacodynamic genome-wide association study identifies new response loci for glucocorticoid intervention in asthma. *Pharmacogenomics J.* 15, 422–429

29 Zhao, W. *et al.* (2005) Structured antedependence models for functional mapping of multivariate longitudinal traits. *Stat. Methods Mol. Genet. Biol.* 4, 1

30 Yap, J. *et al.* (2009) Nonparametric modeling of covariance structure in functional mapping of quantitative trait loci. *Biometrics* 65, 1068–1077

31 Li, N. *et al.* (2010) Functional clustering of periodic transcriptional profiles through ARMA(p,q). *PLoS One* 5, e9894

32 Davidson, S. (2000) Research suggests importance of haplotypes over SNPs. *Nat. Biotechnol.* 18, 1134–1135

33 Li, Q. and Wu, R.L. (2009) A multilocus model for constructing a linkage disequilibrium map in human populations. *Stat. Appl. Genet. Mol. Biol.* 8, 18

34 Sui, Y.H. *et al.* (2014) A case-control design for testing and estimating epigenetic effects on complex diseases. *Brief. Bioinform.* 15, 319–326

35 Li, X. *et al.* (2014) A model for family-based case-control studies of genetic imprinting and epistasis. *Brief. Bioinform.* 15, 1069–1079

36 Li, J.H. *et al.* (2012) The Bayesian lasso for genome-wide association studies. *Bioinformatics* 27, 516–523

37 Jiang, L.B. *et al.* (2016) Evo-Devo-Epi*R*: a genome-wide search platform for epistatic control on the evolution of development. *Brief. Bioinform.* 18, 754–760

38 Jiang, L.B. *et al.* (2015) 2HiGWAS: a unifying high-dimensional platform to infer the global genetic architecture of trait development. *Brief. Bioinform.* 16, 905–911